Predicting the impact of global warming on the timing of spring flowering

INTERNATIONAL JOURNAL OF CLIMATOLOGY
Int. J. Climatol. **30**: 1599–1613 (2010)
Published online 3 September 2009 in Wiley Online Library
(wileyonlinelibrary.com) DOI: 10.1002/joc.2004

RMetS
Royal Meteorological Society

Predicting the impact of global warming on the timing of spring flowering

Robert Malcolm Clark[a]* and Roy Thompson[b]
[a] *School of Mathematical Sciences, Monash University, Clayton, PO Box No. 28M, Victoria 3800 Australia*
[b] *School of GeoSciences, The University of Edinburgh, Edinburgh EH9 3JW, UK*

ABSTRACT: Many plants flower in response to a change in the environment. Since one of the main goals for a plant is to complete a growth cycle in order to produce seed, flowering is a key stage in plant development. We have developed a statistical procedure for explaining the variations in flowering date, which is based on a well-accepted phenological model (growing degree-days). Our approach has several advantages over previous methods based around multiple-regression procedures, the main one being that we have a direct interpretation in terms of just two meaningful phenological parameters (thermal requirement and thermal threshold) per species. The model is used to classify 79 flowering plants. By using a statistical approach based on empirical p-values, we can decide which species can be regarded as sensitive to temperature. Our model, while a simplification of the real system, is easy to work with and enables the consequences of future temperature change to be predicted. By adopting a simple (linear), but realistic, approximation to the rise in temperature each spring, we derive a simple expression for the change in expected flowering dates under global warming. We use the expression to examine changes under three different climate change scenarios involving increasing warmth, oceanicity and continentality. Variations in flowering from species to species and year to year are explained in a straightforward manner by variations in our two parameters and the linear temperature functions, respectively. We find that the sensitivity of spring flowering dates to temperature is strongly governed by the continentality of the climate. We make predictions that will allow the assumptions used in constructing our model to be validated or repudiated. Our formulae can be used for any global warming scenario of the type we consider, whenever our basic assumptions hold. In particular, we predict the likely change in world-wide spring flowering dates under the likely climatic conditions in the 2080s as predicted under the Intergovernmental Panel on Climate Change scenario A1FI. Copyright © 2009 Royal Meteorological Society

KEY WORDS global warming; climate change; onset of spring; phenology; first flowering; statistical model; growth degree-days

Received 20 November 2007; Accepted 20 November 2007

1. Introduction

The growth and development of most plants is highly regulated by the march of the seasons (Battey, 2000). In order to maximise fitness, plants in temperate regions regulate the timing of bud burst and flowering in spring, and the timing of the onset of dormancy in autumn, by adapting to their local annual climatic variations (Häkkinen *et al*., 1998; Saxe *et al*., 2001; Tanja *et al*., 2003). The flowering of a temperate plant is a central event in its yearly cycle. Although the initiation of flowering is typically mediated through the synthesis of flowering hormone by changes in day-length (Salisbury, 1963), the time required for flowers to open and develop to maturity is often strongly dependent upon temperature. Phenological time series of past events provides one means of assessing the sensitivity of plants to various environmental cues (Menzel and Fabian, 1999; Sparks and Carey, 1995; Penuelas and Filella, 2001; Fitter and Fitter, 2002; Hudson *et al*., 2005). The role of temperature, in temperate regions, is often dominant in phenological studies (Fitter *et al*., 1995; Grierson 1995; Oliveira, 1998), as temperature is a fundamental factor that affects the rates of most biological and chemical reactions (Arora *et al*., 2003). Accumulated degree-days, calculated as the sum of the ambient temperatures above a base temperature, provide a measure of biological or thermal time. The concept of growing degree-days is well established having been used for over 200 years (Wang, 1960).

The great Swedish naturalist Carl Linnaeus (1707–1778) initiated the first systematic phenological studies. Phenological observation flourished in the 19th century but then largely fell into neglect until the evidence of climate change, and the desire to understand ecological mechanisms has recently led to a renewed interest (Häkkinen *et al*., 1995; Sparks *et al*., 1997; Chuine *et al*., 1999; Cayan *et al*., 2001). Century-scale instrumental records have demonstrated the occurrence of

* Correspondence to: Robert Malcolm Clark, School of Mathematical Sciences, Monash University, Clayton, PO Box No. 28M, Victoria 3800, Australia. E-mail: malcolm.clark@sci.monash.edu.au

the modern global warming on Earth (Jones and Thompson, 2003). Climate models, ever since the pioneering studies of Manabe (Manabe and Wetherald 1967; Manabe 1970), have consistently pointed to increased global warming with a build-up of CO_2 (IPCC 2007). Observational evidence indicates that regional changes in climate, particularly increases in temperature, have already affected a diverse set of physical and biological systems in many parts of the world (Root *et al*., 2003). Examples of observed changes include shrinkage of glaciers, thawing of permafrost, earlier break-up of ice on rivers and lakes, lengthening of growing seasons, and earlier flowering of plants, emergence of insects, and egg-laying in birds (Parmesan and Yohe, 2003).

We develop a technique to model phenological records of first flowering using the growing degree-days concept. The method is very general. It allows us to predict the effect of global warming on flowering date and generate statistical confidence limits on the projected changes. We use old phenological records from the Royal Botanic Garden Edinburgh (RBGE) to investigate the responsiveness of 79 taxa to mean air-temperature, and to forecast likely changes in their flowering under three global warming scenarios.

2. Materials and methods

2.1. Flowering records

In 1850 McNab started noting the first flowering dates (FFDs) of about 100 spring flowering plants, thus initiating the RBGE tradition of phenological monitoring. Sadler continued recording 40 taxa after McNab's death (1878). Then in the 1900s a new, more extensive, programme saw the monitoring of hundreds of RBGE plants. The bulk of the early 1900s archival material consists of weekly lists of taxa in flower. These observations were made, typically on Thursdays, by the RBGE horticultural staff. From January through to the late summer, the lists are, in general, weekly. In later years the autumn records are only monthly. The main body of data spans the years 1908 through 1938. No observations were made during the First World War (1913–1918). In certain years, the flowering of individual species was not recorded. We attach no particular phenological significance to such minor data gaps. We primarily picked out genera from the archives for which a reasonable number of species had been monitored, e.g. *Saxifraxa* (25), *Prunus* (21), *Geranium* (16), and *Anemone* (13). We further selected 16 species that were in common with taxa studied by Fitter *et al*. (1995). To date, only a selection of the thousands of records of plants monitored at the RBGE have been collated.

Preliminary studies (authors' unpublished calculations) showed an association between FFD and climate. However linkages between last flowering date and climate were otherwise found to be poor. In the ensuing text, we have chosen to concentrate on analysing the relationship between climate and first flowering.

2.1.1. *Editing of data*

To begin with, data for all the species in our chosen genera were digitised from the archives. However, it was soon found that certain taxa had only been monitored for a small number of years. Of the 152 species originally chosen for analysis, 73 were discarded as being unsuitable for statistical analyses, either because there were too few observations or too many FFDs fell outside the range from early spring to early summer for which the linear temperature model was applicable. Specifically, species were deleted if there were more than 4 FFDs less than 75 or more than 4 FFDs greater than 165, or fewer than 12 FFDs between 75 and 165. Our subsequent analyses use data from the remaining 79 species.

2.2. Climate data

Edinburgh has particularly good and extensive records of its weather and climate, with observations of pressure, precipitation, and mean air-temperature extant from 1775 onwards. Sunshine hours, wind, and maximum and minimum temperatures are also available for our period of interest. A preliminary correlation analysis (authors' unpublished calculations) between the flowering data and the meteorological data revealed clear linkages between flowering and mean air-temperature but no consistent relationship with sunshine hours; no major improvement with using maximum or minimum temperature; and little, or no, association with precipitation. Consequently, in the remainder of this paper, we concentrate on the relationship between FFD and mean air-temperatures, examining the extent to which this relationship alone can explain and predict changes in FFDs. Daily mean air-temperature measurements, in Edinburgh, cover the whole of the period of interest to us (1908–1938). These temperatures are the mean daily air-temperature, measured in the shade, using the standard exposure of a louvred white screen at 1.25 m above the ground.

We will be particularly concerned with spring (March to May) temperatures. Year-to-year differences in spring temperatures in Edinburgh can be quite large. Four examples of extreme years are illustrated in Figure 1. Between 1908 and 1938 mean-spring (MAM) temperature in Edinburgh varied from 5.5 to 8.6 °C. Such large interannual variations are a key facet in any procedure designed to use archival records as a basis of predicting future impacts of global warming. The important point is that projected temperature changes are within, or similar to, the interannual range. Consequently, impact predictions do not require any extrapolation beyond the temperature range of the observations.

2.3. Global warming scenarios

2.3.1. *Global climate models and warming scenarios*

Changes in the climate system, in response to increases in greenhouse gases that are confidently predicted, include increases in global mean-surface air-temperature, increases in global mean rates of precipitation, and rising

sea level (IPCC, 2007). However, substantial uncertainties remain in the magnitudes and geographical distribution of the changes and in the rates at which they may be expected to occur. Gyalistras (2002) has reviewed climate change scenarios for Europe. He considers that the climatic evolution of Europe remains uncertain except for the sign of the temperature change and for a general northward drift of the major atmospheric circulation patterns.

We explore the implications of three climate change scenarios on flowering behaviour in Britain. In scenario 1, temperatures are 1 °C higher than normal. Scenario 2A uses the results of local RCMs, e.g. UKCIP98, UKCIP02 based on the Hadley Centre suite of models such as HadRM3 (Hulme *et al*., 2002). Here we assume that the mean temperature will rise by 1.5° on Day 75 and 0.5° on Day 165 with a linear trend in between. Scenario 2B has an overall, year around, warming of 365 degree-days, exactly as for scenarios 1 and 2A, but with a 0.5 °C warming at the start of spring (Day 75) which increases to a 1.5 °C warming by Day 165. So scenario 2B represents a more continental climate in contrast with the more oceanic climate of scenario 2A.

In our global analysis we use general circulation model (GCM) output, for the 2080s, from HadCM3 A1FI in a study of the desynchronisation of the springtime phenologies that may occur between species due to future climate change. HadCM3 is a coupled atmosphere-ocean GCM, and one of the major models used in the IPCC (Intergovernmental Panel on Climate Change), (Gordon *et al*., 2000). It provides us, at each grid square of interest, with output that can be easily used to calculate the two key climatic parameters needed to 'drive' our phenological model. These are: (1) the change in springtime temperature between today and some future date and (2) the rate of increase in springtime temperature in a typical year.

2.4. Statistical assumptions

Our notation and methods can be demonstrated by considering initially just one species. Let μ_i denote its expected or theoretical FFD (in Julian days) in year i, and y_i denote the actual observed FFD in year i, both recorded in units of days relative to Day75 (in view of Equation (3) below). We assume throughout, as in most statistical analyses, that the observed dates differ from the expected dates by 'errors' which are assumed to be approximately normally distributed. In other words:

$$y_i = \mu_i + e_i \tag{1}$$

where the 'error terms' e_i (in units of days) are approximately normally distributed with mean zero and standard deviation σ. This assumption is not crucial, since all of our analyses are based on simulation or bootstrapping.

We consider two models:

Model 1: The species is insensitive to temperature, and always comes into flower on the same day each year.

Hence $\mu_i = \mu_0$, independent of the year i.

Equivalently,

$$y_i = \mu_0 + e_i \tag{2}$$

Model 2: The species comes into flower after β growth degree-days above a threshold or base temperature α.

Records of daily temperature in Edinburgh from 1908 to 1938 indicate that for each year the increase in mean daily temperature from mid-March to mid-June is approximately linear (Figure 1). Consequently, we assume that for days between 75 and 165, the mean temperature on Day x relative to Day 75 in year i is given by the linear equation:

$$T_i(x) = m_i x + c_i \tag{3}$$

With this notation, c_i is the mean temperature on Day 75 and m_i is the rate of increase of temperature in degrees per day. These coefficients are estimated by least-squares regression using the known daily temperatures each year. Test calculations show that the choice of the spring period over which Equation (3) is applied is not critical. For example the astronomical definition of spring of Day 80 to Day 172 could equally well have been used. Equation (3) is the key to our methodology, as it allows a simple and elegant linear solution to the heat unit, or growing degree-day, problem.

Setting γ_i equal to the day on which the temperature first reaches the threshold α, Equation (3) and simple geometry (Figure 2) imply that:

$$\beta = \frac{1}{2} m_i (\mu_i - \gamma_i)^2 \text{ where } m_i\ \gamma_i + c_i = \alpha \tag{4}$$

and hence

$$\mu_i = \sqrt{\frac{2\beta}{m_i}} + \frac{\alpha - c_i}{m_i} \tag{5}$$

We assume that each species has its own α and β; this, together with Equation (5), would explain why in any given year, different species have different FFDs.

2.5. Testing Model 2 versus Model 1

If the mean FFD of the species in question depends on temperature, then Model 2 should be a better fit to the data than Model 1. The usual procedure for comparing the fit of two hierarchical linear models is to use the F-statistic in the corresponding analysis of variance. But our models are not hierarchical. Nevertheless, to test our models, we mimic that standard procedure based on analysis of variance for hierarchical linear models, as recommended by Bates and Watts (1988) and Hastie and Tibshirani (1990). Let RSS_1 and RSS_2 denote the residual sums of squares for Models 1 and 2 respectively, with corresponding degrees of freedom ν_1 and ν_2. Then by analogy with this standard procedure, we compute the pseudo F-statistic:

$$F^* = \frac{(\mathrm{RSS}_1 - \mathrm{RSS}_2)/(\nu_1 - \nu_2)}{\mathrm{RSS}_2/\nu_2} = \frac{\mathrm{RSS}_1 - \mathrm{RSS}_2}{\mathrm{RSS}_2/(n-2)} \tag{6}$$

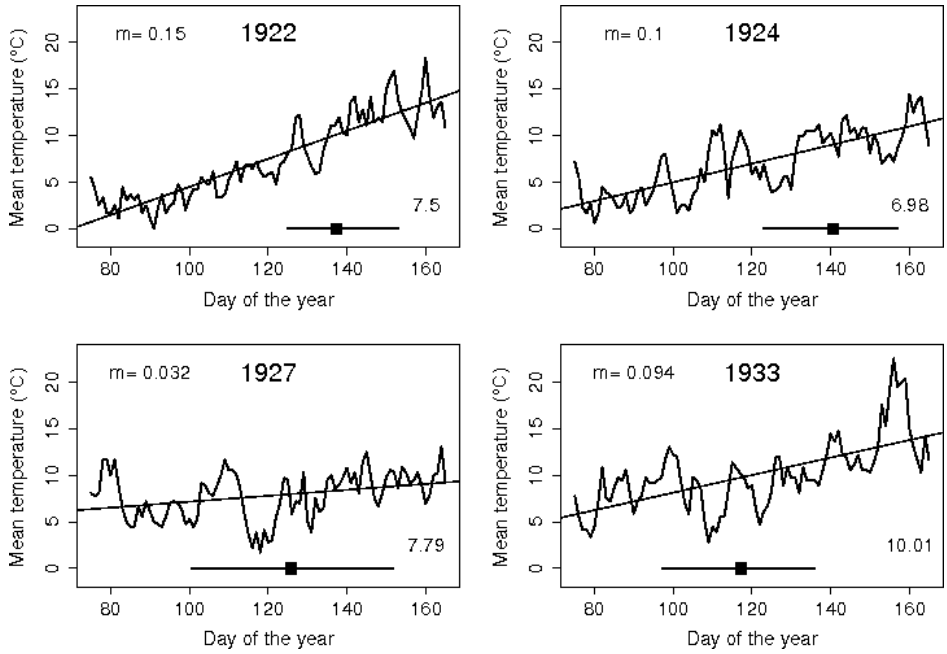

Figure 1. Daily spring air-temperatures in Edinburgh during four representative years between 1908 and 1938. Straight lines are least-squares fits. The gradient of the linear temperature rise (the 'm' in Equation (3)) and the mean temperature in degree celcius are noted in the top left and bottom right corners, respectively. The solid square and bar represent the mean and interquartile range of the FFDs for the 45 species we judge as temperature-sensitive. 1922 is an example of a year in which spring temperatures rise rapidly; 1924, a year of a cold spring; 1927, a year with a very slow rise in temperature; and 1933, a warm spring.

noting that $\nu_1 = n - 1$ and $\nu_2 = n - 2$. If Model 2 is a better fit than Model 1, then F^* should be 'large'. Conversely, if F^* is 'large', it is reasonable to conclude that Model 2 is a better fit than Model 1.

The F-statistic (Equation (5)) does not have the F distribution on 1, $n - 2$ degrees of freedom as might be expected naively. This is for three reasons:

1. The models are not hierarchical (non-nested); i.e. Model 1 is not a special case of Model 2. Although Model 2 has one more parameter than Model 1, Model 2 does not reduce to Model 1 by setting either α or β to zero.
2. Model 2, although linear in α, is subject to the constraint $\beta \geq 0$. This basic constraint cannot be removed by re-parameterising to $\beta^* = \sqrt{\beta}$; while this makes Model 2 linear in both parameters, there is still the constraint that $\beta^* \geq 0$.
3. F^* can be negative. This can happen if Model 1 is in fact true, with small residual variation.

Whilst several alternative tests have been proposed for comparing non-nested hypotheses in regression models (Pesaran, 1982; Godfrey and Pesaran, 1983), these procedures apply only asymptotically, and do not apply when the regression parameters are constrained. In view of these complications, the only way of assessing the significance of an observed value of Equation (6) is by obtaining an empirical p-value by simulation, treating Model 1 as the null hypothesis H_0 and Model 2 as the alternative hypothesis H_1. The procedure involves the simulation of data under Model 1 using the values of μ_0 and σ estimated from the actual data. The test-statistic F^* is then computed for each such simulation, and the p-value is estimated by the proportion of 1000 simulated values of F^* that exceed F^{**}, the value of F^* for the actual data.

The null hypothesis H_0 (Model 1) is rejected in favour of alternative hypothesis H_1 (Model 2) if the empirical p-value is less than 0.05, and we classify the species as 'primarily temperature-sensitive'. Otherwise, we conclude that there is insufficient evidence (at significance level 0.05) to reject Model 1 in favour of Model 2.

The above test procedure is then performed for each of the 79 species. We can then judge each species as 'temperature-sensitive' (as defined by Model 2) or not.

This procedure ensures that the type I error rate, the proportion of false positives, is less than 0.05. Essentially, the same procedure can be used to estimate the type II error rate, the proportion of false negatives. This is equivalent to estimating the power of the test, defined by:

$$\text{Power} = \text{Prob}(F^* > F_c^* | \text{Model 2 is true})$$

where F_c^* is the upper 5% point of the null distribution of F^*, for any given choice of the parameters α and β defining Model 2. In principle, the power could be estimated for a range of assumed α and β corresponding to different levels of sensitivity to temperature, producing a power function.

Such computations would be time-consuming, would require arbitrary choices of the parameters, and would be difficult to interpret. Instead, we compute the empirical

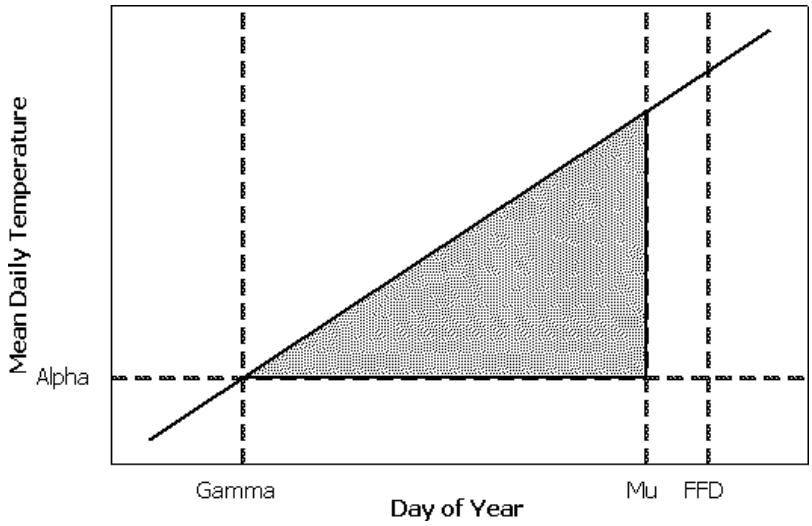

Figure 2. Schematic illustration of our GDD model under our assumption of linear temperature increase, with slope m and intercept c as in Equation (3) for any given species in any given year. Shaded area denotes β, the total thermal days above the threshold temperature α (horizontal line) under the line representing the mean daily temperature. The vertical lines indicate γ, the day on which the temperature first reaches the threshold α and the expected FFD μ under this model. The dashed line denotes the observed FFD, which differs from μ by a 'random error'. This may be positive (as shown here) or negative. The linear temperature function changes from year to year, which is why subscripts are required in Equation (3).

power for just one choice of α and β, namely their estimated values. The empirical power is the proportion of times that the simulated F^* exceeds the critical value F_c^*. Figure 3 gives a schematic illustration of the p-value and power for two representative taxa. The distribution of F^* under Model 2 is always shifted to the right relative to that for Model 1: the relative extent of this shift determines the power. Bisono (2006) showed that our test procedure based on Equation (6) was almost as powerful as those suggested by Pesaran (1982) and others.

2.6. Estimation of parameters

The unknown parameters α and β must be estimated, subject to the obvious constraint that $\beta \geq 0$. When β is significantly greater than zero, standard regression procedures can be used to estimate α and β simultaneously. When β is close to 0, we use the following modified least-squares method. We rewrite Equation (5) as:

$$u_i = \beta^* \sqrt{\frac{2}{m_i}} + \alpha \frac{1}{m_i} + e_i \qquad (5a)$$

where $\beta^* = \sqrt{\beta}$ and $u_i = y_i + c_i/m_i$ (which may be regarded as an 'adjusted' FFD), subject to the obvious constraint that $\beta^* \geq 0$. The method of least-squares is then applied in two stages, by first minimising the error sum of squares with respect to α conditional on a given value of β^*, and then minimising with respect to β^* subject to the constraint.

2.7. Confidence intervals

Rather than presenting the results obtained from solving Equation (5) in terms of the least-squares estimates of α and β and their standard errors, we derive non-parametric bootstrap confidence intervals for each parameter using the bias-corrected and accelerated procedure (Efron and Tibshirani, 1993, Ch. 14; Efron, 1987). We do this for two reasons: first, it is not sensible to give standard errors because of the intrinsic constraint, and second, the non-parametric method makes no assumptions about the distributional form of the data.

2.8. Effect of global warming on mean FFD

How will the expected or average FFD for each species change from the 'present' climate to some 'future' climate?

We represent the present climate by the average linear temperature rise during the spring (mid-March to mid-June). This turns out to be (for Day x relative to Day 75):

$$\overline{T}(x) = 4.4 + 0.09x \qquad (7)$$

We assume that under global warming, the mean temperature on Day 75 increases by A degrees, the temperature on Day 165 increases by B degrees, but otherwise the rate of temperature increase from Day 75 to Day 165 remains linear. The values of A and B are chosen so that the average increase in temperature is 1° over 90 days, making an additional 90 growth degree-days. Let Δ denote the mean difference in expected FFD in the future compared with the present, defined in such a way that $\Delta > 0$ implies that the expected FFD is smaller in the future than in the present, i.e. the plant will flower sooner. Then under Model 2 and this assumption, Δ is given by:

$$\Delta = \sqrt{\frac{2\beta}{M}} + \frac{\alpha - C}{M} - \sqrt{\frac{2\beta}{M + A^*}} - \frac{\alpha - C - A}{M + A^*} \qquad (8)$$

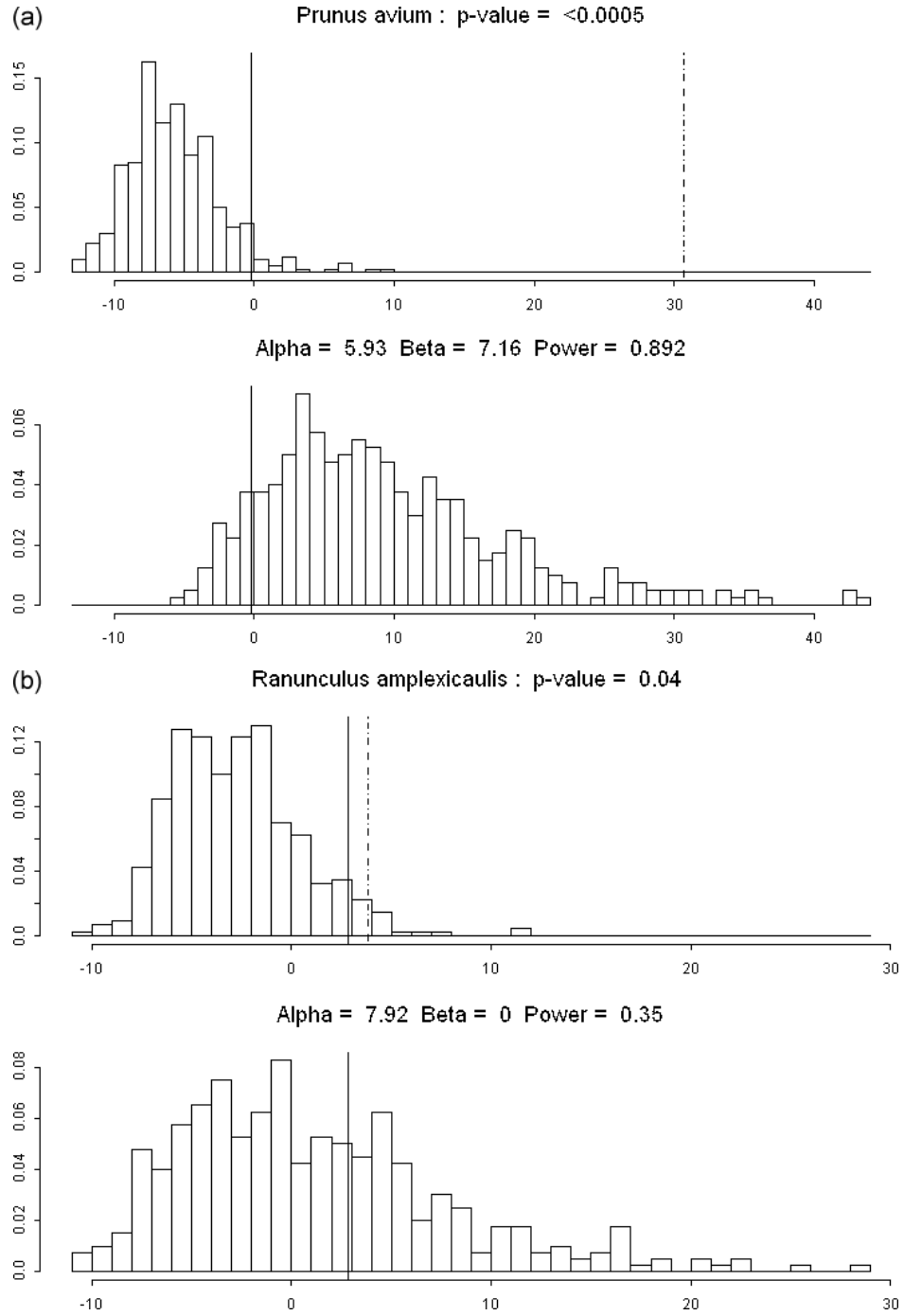

Figure 3. Empirical power and p-value for two representative taxa. For each taxon, the upper histogram shows the simulated distribution of F^* under Model 1, and the lower histogram shows the simulated distribution of F^* under Model 2 using the estimated values of α and β. In each histogram the vertical axis represents proportions, not frequencies, so that the total area under the histogram is 1. The dashed vertical line is the observed value F^{**} based on the actual data, while the solid line is the critical F^*-value F_c^*. In the upper histogram (Model 1), the p-value is the area to the right of the dashed line, and the area to the right of the solid line is 0.05, by definition. The power is the area to the right of the solid line in the lower histogram. (a) *Prunus avium* is an example of a taxon with negligible p-value (high significance) and high power, while (b) *Ranunculus amplexicaulis* is an example with p-value close to 0.05 and low power.

where M and C are the slope and intercept of the average linear temperature relationship (Equation (7)) and $A^* = (B - A)/90$.

2.8.1. *Scenario 1*

The mean temperature increases by 1° uniformly. In other words, $A = B = 1$, and hence A^* in Equation (8) is zero, and consequently $\Delta = A/M = 1/0.09 = 11.1$ days, independently of α and β. In other words, all species will come into flower about 11 days sooner.

2.8.2. *Scenario 2*

Again we assume an overall 1° warming, but for scenario 2A we assume that the mean temperature will increase

by 1.5° on Day 75 and 0.5° on Day 165 (Section 2.3). So in Equation (8), $A = 1.5$, $B = 0.5$ and $A^* = -0.0111$. In scenario 2B, $A = 0.5$ and $B = 1.5$. Since each species has its own α and β, Δ will vary from species to species. We estimate Δ by using the estimated values of α and β in Equation (8). We obtain confidence intervals for Δ for each scenario and each species by applying the same bootstrap procedure as before, but this time using the definition (8) of Δ directly.

2.9. Effect of global warming on the desynchronisation of springtime phenologies

As our phenological model is very general, it can be readily applied to other parts of the world, and to other taxa. In Section 3.1 we use it to estimate the desynchronisation that can be expected between fully temperature-sensitive taxa and temperature-insensitive taxa in temperate climatic regions around the world. In this study, global data from the HadCM3 A1FI GCM was processed as follows. At each grid square of interest, a two-term time-series (1-year + 6-month cycle) was fit to the annual temperature cycle. The time series was used to obtain the day-of-the-year, and magnitude (M) of the maximum rate of increase of temperature. Next, the change of temperature (A) between today and the 2080s, for the day-of-the-year of maximum increase, was derived. Finally, we calculated the ratio A/M.

3. Results

The procedure described in Section 2.5 for testing Model 2 versus Model 1 indicated that 45 of the 79 species were judged to be 'primarily temperature-sensitive' (Table I). α, the growth threshold, averages around 5.8 °C, and ranges from 3.5 °C, for *Saxifraga aizoon* var. *pyrenaica*, to 7.9 °C, for *Ranunculus amplexicaulis* and *R. multifidus* for these 45 temperature-sensitive species. β, the cumulative thermal energy (GDD), averages around 70 degree-days, ranging from zero, for species such as *Anemone rosea* and *A. pulatilla* to 189 degree-days for *Pyrus aria*.

Figure 4 shows the 95% bootstrapped confidence intervals for α and β, plotted against the mean FFD for those taxa judged to be sensitive to temperature. The thermal threshold α is virtually constant while β increases in an approximate quadratic fashion. This relationship is not unexpected. If α is virtually constant and there is relatively small year-to-year variation in the linear temperature relationship, then effectively the subscripts in Equation (4) could be dropped. Then β would be approximately a quadratic function of μ. The confidence intervals for both α and β become wider with increasing mean FFD (equivalently, the estimates of α and β become less precise). This is to be expected since the cumulative thermal energy (GDD) should increase with increasing mean FFD.

Under Model 2, any uniform warming (such as scenario 1) will cause all fully temperature-sensitive species to come into flower the same number of days early. The extent of this change is determined only by the amount of warming (A), and the continentality of the climate (M^{-1}). Figure 5 shows the 95% confidence intervals for Δ, the expected change in the mean FFD under scenarios 2A and 2B as a function of the average FFD, for all our fully temperature-sensitive species. This relationship is approximately linear, since all terms in Equation (8) are approximately linear, noting that β is approximately a quadratic function of mean FFD. Δ depends on both the temperature sensitivity and the magnitude and timing of the warming. Under the more oceanic climate of scenario 2A, Δ decreases through the spring because warming is greater in the winter than in the summer. The small variations about the main trend are caused by differences in β. Plants with large β tend to integrate temperatures over a longer period, and so (in scenario 2A) experience somewhat greater warming than low-β plants which, by virtue of higher αs, happen to have the same mean flowering date. The reduced winter warming of scenario 2B generates smaller changes in FFD. In this case, Δ increases in value through the spring because of the greater warming in summer. In short, Figure 5 illustrates the importance for flowering dates, not only of a warming of the climate but also a change in continentality.

Table I gives the p-value, empirical power, 95% bootstrapped confidence intervals for α, β, and Δ under scenarios 2A and 2B for all 79 taxa, sorted by increasing p-value and then alphabetically. Table I also gives the variability in FFD that remains unexplained by our model, expressed as the residual standard deviation (σ). For temperature-sensitive species, the residual standard deviation generally ranged from 5 to 15 days. As would be anticipated, species we judge as not primarily temperature-sensitive, tend to have higher unexplained variances. However, a number of temperature-sensitive species, e.g. *Geranium cinereum* and *G. phaeum*, also have high natural variability (standard deviations of 19 days) that is not accounted for by temperature. An important task for phenologists is to explain such variability.

Table I also gives the ratio of the unexplained variability in FDD (expressed as residual standard deviation or σ) for Model 2 relative to Model 1. For species that are judged to be sensitive to temperature, this ratio is generally less than 1, as expected.

The power analysis is used to guard against wrongly declaring a species to be not sensitive to temperature. Ideally, we want a test to have high power. A low power warns us that the sample size is too low, and hence our hypothesis test lacks the precision to provide reliable answers. As can be seen in Table I, the power is good for many species such as *Cardamine trifolia* and *Prunus avium*, but surprisingly poor for others such as *Iris florentina*.

3.1. Time resolution of phenological observations

At first sight, a time resolution of 1 week on the phenological observations might seem low for our purposes.

Table I. Statistical properties, and 95% confidence intervals for parameter estimates and climate scenario results, for 79 taxa.

Taxa	*p*-value	Power	α[a] (°C)		β[b] (degree-days)		Δ2A[c] (days)		Δ2B[c] (days)		σ[d] (days)	Ratio
Cardamine trifolia	0	0.527	3.2	7.0	0	79	14.3	17.5	6.1	8.6	14.9	0.78
Prunus avium	0	0.892	3.8	7.0	0	53	14.3	16.9	6.8	8.6	12.2	0.64
Geranium robertianum	0	0.595	3.5	7.1	99	428	11.1	13.7	9.4	11.4	16.7	0.75
Iris florentina	0	0.163	4.0	5.8	126	255	12.0	13.9	9.2	10.1	7.3	0.59
Sorbus latifolia	0	0.233	4.5	6.4	56	216	9.2	13.8	9.2	10.4	7.3	0.52
Cerasus avium	0	0.438	4.4	7.0	0	51	14.1	16.2	7.3	8.9	11.1	0.71
Pr. serrulata	0	0.755	4.2	6.9	11	105	13.5	15.3	8.0	9.2	8.4	0.59
Ranunculus montanus	0.001	0.547	6.6	7.7	0	14	13.2	15.0	8.1	9.4	12.6	0.72
Pr. cerasus	0.001	0.777	3.3	5.9	42	184	14.0	15.8	7.6	8.9	6.8	0.54
Anemone nemorosa	0.002	0.657	5.3	6.7	0	4	14.8	16.3	7.1	8.2	14.6	0.86
Pr. avium cv. 'P. Tricolor'	0.003	0.263	3.8	6.9	0	70	14.2	16.5	7.1	8.7	11.3	0.78
A. rosea	0.004	0.225	5.9	7.1	0	10	14.2	15.3	7.5	8.6	10.9	0.76
Malus baccata cv. 'F. Maximo'	0.004	0.458	3.3	5.9	44	211	13.8	15.3	7.9	9.1	13.7	0.78
Pr. tomentosa	0.004	0.515	6.5	7.4	0	9	14.0	15.1	8.0	8.9	13.5	0.83
A. nemorosa cv. 'Robert.'	0.005	0.403	5.6	6.8	0	0	14.7	16.3	7.1	8.3	13.7	0.95
Pr. persica cv. 'F. Alboplena'	0.005	0.297	4.8	6.9	0	19	14.5	16.0	7.4	8.5	11.7	0.86
I. biflora	0.006	0.210	4.1	8.4	0	148	11.7	15.0	8.3	10.5	8.5	0.80
Saxifraga umbrosa cv. 'Varieg.'	0.006	0.145	1.0	6.3	67	426	12.7	17.0	6.9	10.0	10.9	0.82
So. aucuparia cv. 'Pendula'	0.007	0.008	3.9	6.7	79	246	12.1	14.3	9.0	10.6	8.8	0.89
I. missouriensis	0.007	0.008	3.5	6.8	29	184	12.6	15.1	8.1	10.0	8.2	1.13
So. aria	0.008	0.028	1.3	6.0	140	406	11.9	14.2	9.1	10.7	8.0	0.83
C. pinnata	0.009	0.263	5.3	7.3	0	23	13.8	15.1	8.0	8.9	11.4	0.85
I. siberica	0.009	0.560	5.0	10.0	0	188	9.8	13.2	9.6	12.1	15.9	0.80
Sa. juniperifolia	0.009	0.477	4.7	6.3	0	0	15.5	17.1	6.4	7.7	14.2	0.96
So. aucuparia cv. 'Fifiana'	0.009	0.030	3.8	6.8	84	257	11.8	14.3	8.9	10.5	9.0	0.95
G. phaeum	0.010	0.385	2.5	9.3	10	428	10.5	15.1	8.4	12.0	19.3	0.84
So. alpina cv. 'Superaria'	0.010	0.058	4.2	6.6	71	225	12.2	13.8	9.1	10.4	9.1	0.85
Pyrus salicifolia	0.010	0.398	4.2	7.4	0	58	13.0	16.3	7.1	9.1	13.0	0.86
R. auricomus	0.011	0.170	2.9	7.3	0	111	13.8	16.3	7.2	9.0	12.7	0.88
M. spectabilis cv. 'Rosea'	0.011	0.323	2.7	6.3	23	239	13.1	15.9	7.6	9.5	14.5	0.83
M. spectabilis	0.016	0.335	1.1	7.4	7	405	13.2	17.0	6.5	9.4	16.0	0.84
M. baccata	0.018	0.338	2.6	6.2	35	267	14.0	16.5	7.2	9.0	15.0	0.85
Py. pinnatifida	0.018	0.228	1.7	6.9	65	371	12.3	16.4	7.3	10.3	9.1	0.80
Sa. umbrosa	0.019	0.130	3.6	7.8	11	215	11.9	15.0	8.3	10.7	13.7	0.93
I. bucharica	0.021	0.215	5.4	7.4	0	16	13.8	15.9	7.5	9.0	13.1	0.97
R. gramineus	0.021	0.150	4.9	8.8	0	94	11.6	14.7	8.6	10.6	13.9	0.94
Sa. ciliata	0.021	0.380	5.6	6.3	0	0	15.4	16.6	6.9	7.8	13.0	0.91
M. floribunda	0.024	0.228	3.6	7.2	2	146	13.3	15.7	7.5	9.4	14.9	0.92
Pr. mahaleb cv. 'Globosa'	0.024	0.090	5.3	7.6	9	96	11.9	14.0	9.0	10.3	10.5	0.80
A. pulsatilla	0.027	0.328	5.7	6.4	0	0	15.4	16.5	6.9	7.8	13.1	1.04
Pr. cerasus cv. 'Pulverulenta'	0.027	0.258	1.1	6.5	36	392	13.3	17.8	6.4	9.5	12.9	0.87
Pr. armeniaca	0.033	0.245	5.8	6.9	0	13	14.6	16.2	7.0	8.4	15.8	0.99
R. acris	0.035	0.093	3.9	7.3	22	193	12.5	15.0	8.4	10.3	11.3	0.96
M. baccata cv. 'Hiemalis'	0.035	0.250	2.4	7.6	5	230	12.9	16.7	7.0	9.3	16.6	0.83
R. amplexicaulis	0.040	0.350	7.3	8.4	0	16	12.3	13.8	9.1	10.1	15.2	0.91
R. multifidus cv. 'Fl. Pt.'	0.044	0.078	5.1	9.0	0	82	11.3	14.5	8.8	11.0	12.5	0.96
I. neglecta	0.045	0.150	2.8	9.0	27	398	9.7	14.4	8.9	12.3	12.7	0.91
G. macrorrhizum	0.049	0.258	0.4	8.5	56	804	9.7	16.3	7.6	12.0	15.4	0.85
A. pulsitilla cv. 'Amoena'	0.054	0.300	5.4	6.4	0	0	15.3	16.8	6.7	7.8	11.6	1.21
M. sieboldii	0.060	0.230	0.3	6.6	20	458	13.2	17.9	5.9	9.5	17.7	0.90
So. aucuparia	0.062	0.053	2.4	5.3	156	407	12.8	15.3	8.1	9.9	11.3	0.99
M. x prunifolia	0.062	0.212	2.0	7.6	8	266	12.5	16.9	6.9	9.6	16.8	0.91
Pr. mollis	0.068	0.015	4.8	8.4	6	106	11.5	14.4	8.8	10.7	11.1	1.11
I. orientalis	0.073	0.170	−1.1	6.8	126	597	10.7	15.5	7.4	11.6	16.3	0.90
M. orthocarpa	0.100	0.102	2.2	7.3	7	284	13.1	16.8	6.9	9.6	16.4	0.96
Primula sikkimensis	0.101	0.083	4.5	8.1	26	230	11.3	13.8	9.3	11.2	14.5	1.02
A. alpina	0.116	0.005	5.5	8.6	0	60	11.6	14.3	9.0	10.7	11.7	1.26
Sa. allionii	0.125	0.073	3.7	9.0	0	159	11.0	15.2	8.2	11.2	17.1	0.98

Table I. (*Continued*).

Taxa	*p*-value	Power	α[a] (°C)		β[b] (degree-days)		Δ2A[c] (days)		Δ2B[c] (days)		σ[d] (days)	Ratio
Sa. afghanica	0.126	0.383	4.0	7.1	0	131	14.1	17.0	6.1	8.6	24.2	0.97
Pr. mahaleb	0.131	0.010	4.1	8.5	0	133	12.0	15.1	8.3	10.5	12.7	1.05
Pr. triloba	0.133	0.145	4.6	6.4	0	17	15.4	17.2	6.2	7.9	18.4	1.16
I. ruthenica	0.156	0.025	3.5	8.0	31	252	11.7	14.8	8.4	11.0	11.3	1.06
So. aucuparia cv. 'D. Aurea'	0.166	0.010	2.7	6.7	77	335	11.0	14.8	8.5	10.9	10.8	1.35
Euphorbia amygaloides	0.168	0.153	4.9	7.5	0	34	13.5	16.4	7.0	9.2	20.7	1.02
Py. conescens	0.169	0.255	2.1	7.7	0	155	13.3	18.1	5.9	9.4	18.9	0.98
Sa. wallacei	0.192	0.145	4.1	8.8	0	137	11.4	15.2	7.9	10.9	17.8	1.00
Pri. veitchii	0.221	0.030	3.9	8.4	0	124	12.0	15.9	7.8	10.5	15.3	1.11
Sa. trifida	0.229	0.180	4.4	8.9	0	172	11.6	14.9	8.5	10.8	14.8	0.95
Sa. decipiens	0.234	0.183	7.4	8.7	0	63	11.6	13.4	9.2	10.6	19.7	1.01
A. sylvestris	0.237	0.142	2.3	6.9	45	381	12.1	15.4	6.6	10.5	14.5	0.98
Aronia arbutifolia	0.279	0.003	4.5	8.5	45	245	10.1	13.2	9.8	12.1	9.2	1.34
Acer campestre	0.312	0.018	3.2	8.7	0	201	11.5	16.1	7.8	10.7	15.6	1.13
Pri. allionii	0.336	0.138	5.4	6.6	0	0	15.0	16.8	6.6	8.0	17.0	1.18
Pri. cockburniana	0.336	0.018	4.7	8.6	9	204	11.0	13.5	9.3	11.1	14.6	1.16
R. ficaria cv. 'Alba'	0.336	0.145	5.3	7.1	0	24	14.1	16.6	6.8	8.7	22.9	1.14
Pr. persica cv. 'Pyramidalis'	0.420	0.075	5.7	7.0	0	0	14.2	16.4	7.1	8.7	12.4	1.56
Pr. amygdalus cv. 'Georgica'	0.501	0.025	6.8	7.7	0	45	13.2	14.8	8.2	9.4	16.2	1.31
Sa. lingulata	0.770	0.313	7.6	9.6	0	41	10.4	14.0	8.9	11.5	39.3	1.03
Py. communis	0.847	0.058	1.7	9.1	0	279	10.8	16.2	6.7	11.2	29.9	1.14

Taxa names follow the RBGE nomenclature used in the early 1900s.
As the true *p*-value could be marginally greater than the empirical (simulated) values listed in column 2 (as judged by a hypothesis test for a binomial proportion), we use a value of 0.040 (rather than 0.05) to distinguish between Models 1 and 2. The 45 species with *p*-value of 0.040 or less (those above the solid horizontal line), are taken to be primarily temperature-sensitive.
Last column gives the ratio of unexplained variability of Model 2 relative to that of Model 1.
[a] α is the thermal threshold.
[b] β is the thermal requirement.
[c] Δ is the expected or predicted change in mean FFD under model 2A or 2B.
[d] σ is the unexplained variability (residual standard deviation under Model 2).

We therefore carried out several analyses to determine the influence of different time resolutions on our calculations. To do this, we made use of daily observations of FDDs at the same Botanic garden site made during the late 1800s. We applied our degree-day procedures to the daily observations, to the daily observations degraded to weekly values, and to fortnightly values. In particular, we compared the accuracies (and parameters) derived from the actual daily phenological observations with those derived from the weekly and fortnightly observations. We found no significant differences. These calculations demonstrate that weekly values are quite satisfactory for our purposes. In retrospect, the reason why a lack of daily observations has only a minor effect on our results

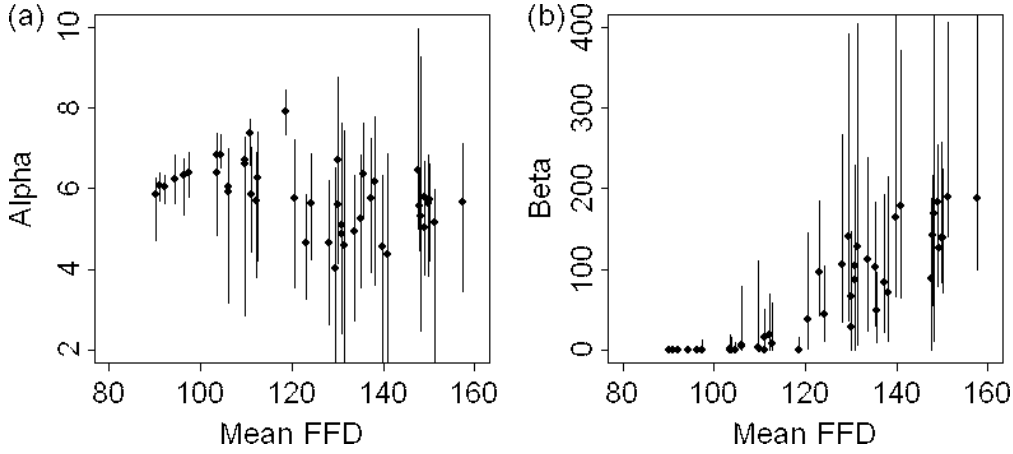

Figure 4. Confidence intervals for α and β. Estimated values plus 95% bootstrapped confidence intervals for (a) α and (b) β, respectively, plotted against the mean FFD (the estimate of μ_0 under Model 1).

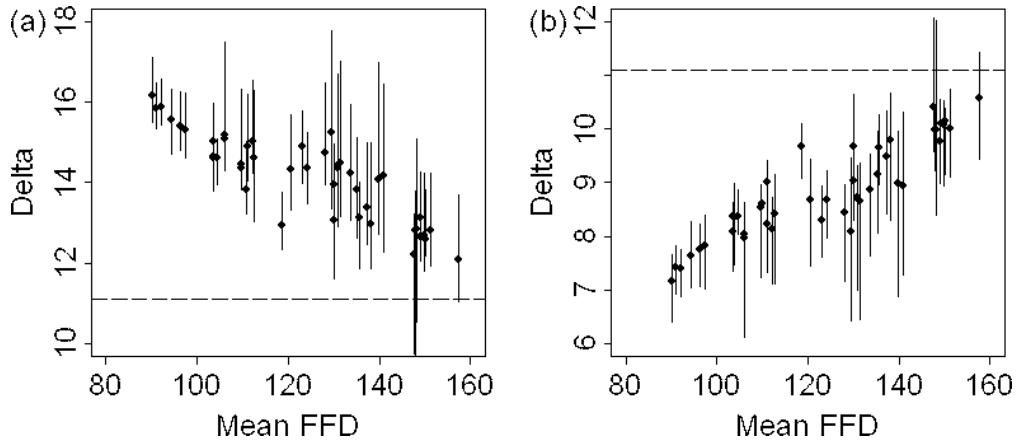

Figure 5. Impact of global warming (scenarios 2A and 2B) on FFDs. Estimates and 95% bootstrapped confidence intervals for Δ, the expected or predicted change in mean FFD under (a) scenario 2A and (b) scenario 2B. Horizontal line corresponds to scenario 1. The confidence limits are not symmetric due to the constraint on β. The vertical bars do not indicate interannual variability, just the uncertainty in estimating Δ from small samples.

can be explained as follows. First, the residual error in our basic equation is the sum of a 'model error' and the 'measurement error'. The latter follows a uniform distribution on 0, 1, . . ., 6, which has mean 3 and variance 4. Now we find that the standard errors of our predicted FFDs, according to our GDD model, are mostly around 11 days, but can be as low as 7.5 days in some cases. Since variances, not standard deviations, add up, the measurement error has variance 4 out of a total variance of typically 50–120 or more, and so, is of relatively minor importance. Second, recording leafing, or FFDs, to a true accuracy of just 1 day is difficult to achieve in practice because different observers can be involved, and observing a large plant or tree is not necessarily straightforward. Third, plants respond to the weather when integrated over several weeks, if not months, rather than just in 1 or 2 days immediately before leafing or flowering. In summary, while it would be nice to have accurate, daily FFDs, such information, over and above weekly observations, is of limited practical value for our purposes.

3.2. Uniformity of parameters

One of our aims is to apply our phenological model to the analysis of desynchronisation of springtime phenophases over the world. As a preliminary, a demonstration of the geographical uniformity of the values of the parameters α and β for individual temperature-sensitive species could be useful. The conceptual relationship between α, β, and the local climate has been shown in a previous study (Thompson and Clark, 2006, Figure 3). In particular, we showed that the sensitivity of FFD, or flushing date, to temperature depends on the rate of increase of springtime temperatures and not on the precise temperature threshold, or GDD requirement. In this respect, we checked the uniformity of our degree-day models across two main data sets. These are: (1) pan-European phenological observations on natural populations of *Pr. padus* (293 observations) and *Tilia cordata* (1705 observations) (Thompson and Clark, 2006) and (2) extensive observations on clonal trees in the International Phenological Gardens (Chmielewski and Rötzer, 2001) (our unpublished calculations). In both cases, we find no evidence for a significant variation of the degree-day parameters with geography. Instead, we find our phenological models apply across regions spanning hundreds of thousands of square kilometres.

3.3. Desynchronisation of springtime phenologies

Figure 6 plots the desynchronisation that can be expected around the world by the 2080s, based on our phenological model, the IPCC emission scenario A1FI, and the HadCM3 global circulation model. The map plots Δ of Equation (8) and represents the difference between the change in flowering date of thermally sensitive and photosensitive taxa to a change in the local climate. Δ was calculated on a 0.5×0.5 degree grid; it is given by the ratio of the change in springtime temperature, A, and the rate of increase of spring temperature rise, M. Desynchronisations range from under 10 to over 50 days. Regions with no vegetation (polar ice, inland waters, desert) or moisture dominated phenologies (savanna, semi-desert, thorn woods, salt flats), or with little or no seasonal temperature change (tropical and subtropical biomes) have all been left blank. Each grid square shows the ratio A/M, which is our estimate of the difference in response between temperature- and photoperiod-sensitive taxa.

Mainly, as a consequence of the strong continentality (high M) of their climates the interiors of the Northern Hemisphere land masses are predicted to show only modest desynchronisation. So although climate warming is expected to be large over the northernmost edge of the northern continents, we estimate that large tracts of land from the Urals eastwards right across north-east Asia to Alaska, the Yukon, and Manitoba will experience little between taxa desynchronisation. In contrast strong desynchronisation is modelled for west-coast maritime climates (e.g. the coastal ranges and mountains of British Columbia and Washington State, the Atlantic

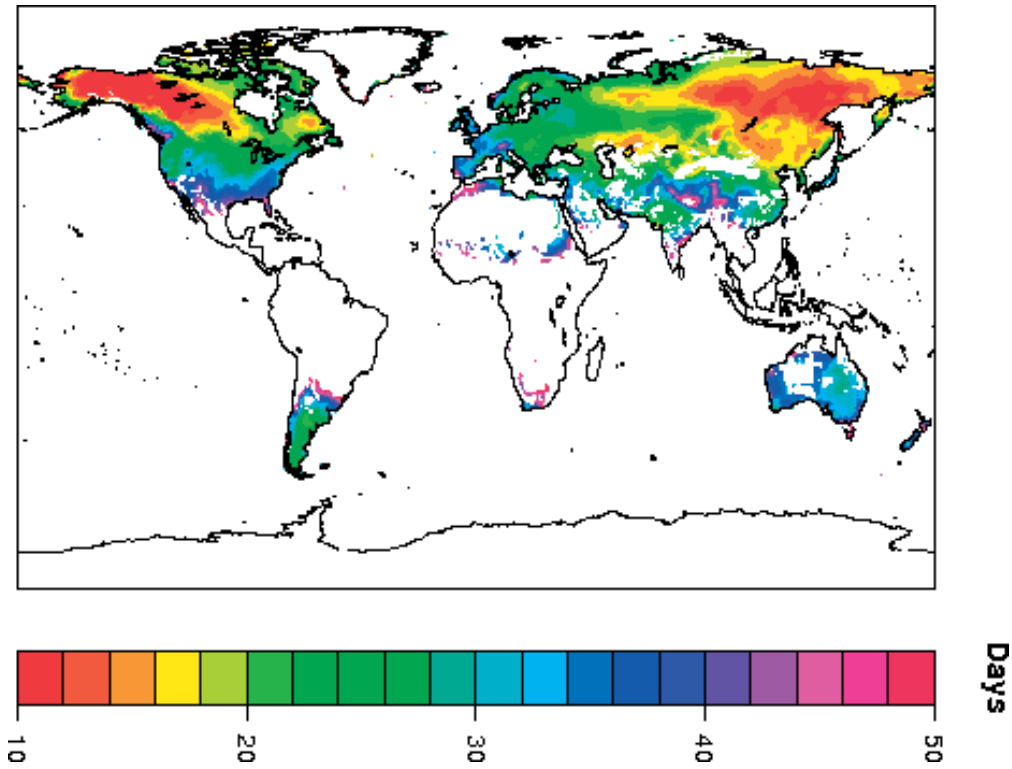

Figure 6. Phenological desynchronisation expected under IPCC global warming scenario A1FI for the 2080s. The map plots Δ of Equation (8) and represents the difference in the change of flowering date of thermally sensitive and photosensitive taxa to a change in the local climate. Δ was calculated on a 0.5×0.5 degree grid. It is given by the ratio of the change in springtime temperature, A, and the rate of increase of springtime temperature, M.

hinterlands of Western Europe and North Africa, New Zealand, Western Australia, Western Chile) and for lower latitude biomes with temperature-dependent phenological components. Phenological information about lower latitude taxa is rather scarce. Nevertheless, specific examples of temperature-sensitive phenologies in lower latitude biomes are the Arizona-Sonora desert (Bowers and Dimmitt, 1994; Bowers, 2007), the Australian Box-Ironbark eucalypt forest (Keatley and Hudson, 2007), and *Eucalyptus regnens* eucalypt forests in southeast Australia (Keatley's 10-year record of unpublished data and author's unpublished calculations). Pronounced desynchronisation can be anticipated in warm temperate, subtropical or oceanic regions such as Florida, the western Mediterranean, western Australia, Indo-Burma, and New Zealand. It is salutary to note that all five of these strong desynchronisation regions coincide with biodiversity hotspots (Figure 1 in Myers *et al*., 2000), where endemic species are currently undergoing exceptional loss of habitat and so already constitute priority habitats for conservation planners.

4. Discussion

4.1. Caveats on the limitations of our approach

It is important to note the simplifications we have adopted in our statistical analysis. We have assumed that: (1) the rate of increase of temperature between mid-March and mid-June in any year is linear, (2) the thermal degree-days depend only on the mean daily temperature (independent of the daily minimum, maximum, or hours of sunshine), and (3) the global warming effect is quantified by a linear change in temperature, relative to the average linear temperature change over the 31 years considered.

Assumption (1) seems reasonable, as indicated by the four typical years shown in Figure 1. Furthermore, it is well established that spring flowering dates are often associated with air-temperatures 1, 2, and 3 months prior to flowering (Fitter *et al*., 1995; Sparks *et al*., 2000), and not just to temperatures at the time of flowering. So a method, like ours, which integrates air-temperatures over a period of several weeks, can perform well. Indeed, the simplicity of the basic method allows it to outperform more complex methods. At first sight a method using daily temperature data would be expected to be more skilful than the one using monthly, or longer, averaging. However, the slight loss of temperature information in our linear model is more than compensated by the avoidance of threshold effects, non-linearities, and problems connected with finding the true global minimum during optimisation. Kramer (1994) highlights the difficulties that methods using daily forcing can encounter. He reviews 12 different phenological models with up to 12 free-parameters, but found that only one managed to outperform the null model (the mean). We too found that use of daily data provided only very minor improvements to fit but had the major

disadvantage of precluding confidence limit and power calculations.

In principle, it is straightforward to obtain prediction limits for FFDs of a given species in given years, applying well-known results from linear regression (Seber, 1977, chapter 7) The width of these prediction intervals depends on both the slope and intercept of the temperature gradient and the residual σ, given in Table I. Hence it is not possible to give an overall statement of the precision of predicted FFDs.

Residual plots for our selected models were (generally) satisfactory, as were plots of observed versus predicted FFDs, with no real difference between significant and non-significant species, except for obvious greater spread in the latter. In addition, our procedure has been validated by our extended analysis using 1706 observed FFDs of *Pr. padus* and 294 observed FFDs of *T. cordata*, from a range of locations, with latitudes varying from 45°N to 70°N (Thompson and Clark, 2006).

Regarding assumption (2), a preliminary analysis of the available meteorological data for Edinburgh showed that hours of sunshine were only weakly correlated with the daily mean temperature. Nevertheless, inclusion of daily minimum, maximum, or hours of sunshine did little to improve our approach.

A further assumption we are making is that the linear temperature increase is appropriate to both the 'past' and the 'future'.

The restricted range of species we are able to analyse also limits our approach. We have to pre-select spring flowering species. These taxa however dominate the RBGE living collection.

4.2. Generalisation

Our method is a general approach applicable to any situation where the FFD of a spring flowering species depends primarily on the total thermal days above a threshold temperature. Equation (8) can be used to predict the effect on the mean FFD for a particular species for any global warming scenario of the form considered here, i.e. any values of A and B in Equation (8).

To what extent can our results be generalised: To other climatic regions? To other 'similar' taxa? Equation (8) is applicable to any (linear) global change and so potentially applicable to a wide range of situations. Under our climate scenario 1 of uniform temperature change throughout the year, all fully temperature-responsive species conform to one another and display only one response. In all cases the response will be M^{-1} days/°C and is the same for all 'temperature-responsive' species. (We exploited this generalisation in the construction of Figure 6.) Under scenario 2, all fully temperature-responsive plants that flower at the same time of year show very similar responses to changing temperatures. Under scenario 2A, temperatures increase more in early than late spring, and so an enhanced temperature response is predicted for earlier flowering species. In contrast under scenario 2B, early spring temperatures change less (although the overall annual temperature increase is the same in all the scenarios we consider) and hence we predict a reduced temperature response for earlier flowering species. We speculate that plants from the temperate zone that are predominantly responsive to springtime temperature will all follow these general behavioural patterns. Plants within a geographical region will be attuned to their local climate. We predict greater temperature responses in oceanic climates (like Scotland) where spring temperatures rise slowly (M^{-1} is high) and weaker responses in continental climes (continental interiors) where spring temperatures rise rapidly (M^{-1} is low).

In more tropical regions the phenology of flowering, fruiting, and leafing can be very different to that in temperate climates; it can involve multiple flowerings and stronger relationships to precipitation (Bawa *et al*., 2003; Keatley *et al*., 2004), and hence these regions were excluded from our desynchronisation studies.

4.3. Comparison with correlation and regression analyses

Our approach is based on a known phenological model for the growth of plants rather than a regression fit to past data on FFDs. While such regression procedures often give a reasonable fit (Fitter *et al*., 1995; Sparks and Carey, 1995; Sparks *et al*., 1997), they give no explanation for such results and do not extrapolate naturally to other species or future data. Multiple regression has a number of drawbacks. In phenological studies, there are often many plausible but highly correlated explanatory variables and relatively few years of observations. There are well-known procedures for selecting subsets of correlated regressors, such as stepwise regression and best subsets regression (Miller, 1984). Nevertheless in cases such as these, the fitted regression equations are typically unstable. If, for instance, one particular regressor is omitted, then there can be significant changes in the coefficients of the remaining regressors. This is why the interpretation of regression equations is fraught with danger. Further, with few years of observations, multiple-regression techniques can have low power, because of low degrees of freedom for error. In contrast, our procedure avoids the drawbacks of multiple regression and uses a simple model involving two easily interpreted parameters, leading to an enhanced scope for prediction and generalisation.

For species with $\beta = 0$ in our GDD model, this does not mean that they have not experienced any temperatures above that of the thermal threshold. The temperature of plant tissue and the air inside a meteorological screen are very different. Furthermore, each day a plant undergoes a cycling of its temperature due to diurnal fluctuations in insolation and air-temperature. $\beta = 0$ means that the first flower opens on the day when the linear rise in springtime temperature reaches α.

4.4. Comparisons of phenological data from one century to the next

At first sight it might seem possible to validate our prediction method by hindcasting past phenological changes and comparing them with observations. For example one could compare phenological observations made in the Royal Botanical Garden in Edinburgh in the epoch beginning in the 1850s (Harper *et al*., 2005) with those analysed here (from 1908 to 1938), and with those obtained on a newly re-established monitoring programme (2002 onwards) (Harper and Morris, 2006). Unfortunately, there are three difficulties. First, although hundreds of taxa were monitored in the early 20th century, only a few of these were monitored in the 1800s. Second, temperatures changed only by a fraction of a degree between each of these periods so that any phenological signals are likely to be rather small. Third, when the few matching taxa are compared their flowering dates are commonly seen to have changed dramatically (often by several weeks). Some become earlier, others later, while a few change only a modest amount. In retrospect, it seems likely that any climate change signal has become swamped by additional effects. Here a likely explanation is that the plants themselves have changed over the centuries so that their phenological data are no longer directly comparable. For example the cultivars, or the precise varieties, could have altered. It is because of this type of difficulty that our preference for predicting future phenological changes lies with calibrating phenological models using interannual changes. The main advantages are that temperature changes from year to year can be large, and any long-term changes in plant genotype can be avoided.

4.5. Improved models

The method outlined above is very general and so can be readily extended to include additional effects. For example the budding and flowering of many temperate trees are affected by wintertime chilling (Campbell *et al*., 1975; Häkkinen *et al*., 1995; Häkkinen *et al*., 1998) as well as by springtime warmth. Chilling can be incorporated into our basic model by expanding β in Equation (4) in order to make it depend on chilling duration (Thompson and Clark, 2008).

Our model could be improved by combining a photoperiod effect along with a thermal effect. This leads to a three-parameter model that can be examined in essentially the same way as our two-parameter model. Preliminary studies have led to only modest improvements in fit. Similarly, Kramer (1994) has found that more complex phenological models do not necessarily perform better than simple models.

Thompson and Clark (2006) give a general theoretical framework to GDD models that incorporates both a photoperiod effect and a general monotonic increase in daily temperature. Both a linear function and suitably restricted sinusoidal function are special cases of such a monotonic function.

At first sight it might be expected that the use of individual daily temperatures, rather than our linear fit to spring temperature rise, would improve the modelling. Unfortunately, modelling using daily data necessitates optimisation methods. Extensive trials produced no significant improvements in fit and caused major difficulties in the construction of confidence intervals (on account of multiple local minima). In retrospect, the good performance of the linear approach is seen to arise because the main mechanisms controlling flowering times integrate temperatures over a period of many weeks.

Another improvement would be to represent temperature change each year as a sine function (Allen, 1976). Our current assumption of linearity of temperature increase between mid-March and mid-June corresponds roughly to the approximate linear part of this sine curve. Test calculations indicate that when dealing with temperature changes between about -3° and $+3^{\circ}$, the differences caused to our analyses between a sine function and linear fit approach are minimal (Thompson and Clark, 2006). The main advantage of a sine-function approach would be that our method could also be used with winter flowering plants.

5. Conclusions

- A general linear modelling method, based on thermal degree-day growth, allied with an assumption of a linear change in spring temperature, has been developed to model FFDs.
- Spring FFDs in Edinburgh show a good association with air-temperature. We find that 45 out of 79 taxa are primarily temperature-sensitive.
- We demonstrate that the sensitivity of spring flowering dates to temperature is strongly governed by the continentality of the climate.
- We predict high temperature sensitivities of flowering in oceanic climates, and in low-latitude, temperate biomes.
- We illustrate our method by predicting the changes in spring flowering to be anticipated in Scotland for three climate change scenarios. All three scenarios are based on an average 1 °C temperature rise. For scenario 1 (1 °C increase throughout the year), we predict a shift in the botanical season of approximately 11 days with respect to the climatic year. For scenario 2A (greater winter than summer warming), we predict shifts ranging between 16.2 days at the start of spring and 11.2 days at the end of spring. For scenario 2B (a warmer, more continental climate), we predict shifts ranging between 7.2 days at the start of spring and 11.2 days at the end of spring.

Acknowledgements

We thank D. Mann for drawing the Edinburgh phenological records to our attention, the RBGE library staff for their help in facilitating access to the original data, and G. Harper for discussions on flowering,

RBGE history, and on horticultural practice and nomenclature. Undergraduate students on the Edinburgh University Environmental Geosciences and Geophysics Honours degree courses helped collate the flowering data. HadCM3 data were obtained from IPCC's comprehensive Data Distribution Centre (DCC) <http://www.ipcc-data.org/sres/hadcm3_download.html>

References

Allen JC. 1976. A modified sine wave method for calculating degree days. *Environmental Entomology* **5**: 388–396.

Arora R, Rowland LJ, Tanino K. 2003. Induction and release of bud dormancy in woody perennials: A science comes of age. *HortScience* **38**: 911–921, DOI: 10.1071/FP0627.

Bates DM, Watts DG. 1988. *Nonlinear regression analysis and its applications*. Wiley: New York.

Battey NH. 2000. Aspects of seasonality. *Journal of Experimental Botany* **51**: 1769–1780, DOI:10.1093/jexbot/51.352.

Bawa KS, Kang H, Grayum MH. 2003. Relationships among time, frequency, and duration of flowering in tropical rain forest trees. *American Journal of Botany* **90**: 877–887.

Bisono IN. 2006. *Comparison of tests of non-nested hypotheses with application to phenology*. M Sc. Thesis, Monash University.

Bowers JE. 2007. Has climatic warming altered spring flowering date of Sonoran Desert shrubs?. *Southwestern Naturalist* **52**: 347–355.

Bowers JE, Dimmitt MA. 1994. Flowering phenology of six woody plants in the northern Sonoran Desert. *Bulletin of the Torrey Botanical Club* **121**: 215–229.

Campbell RK, Sugano AI. 1975. Phenology of bud burst in Douglas-fir related to provenance, photoperiod, chilling and flushing temperature. *Botanical Gazette* **136**: 290–298.

Cayan DR, Kammerdiener SA, Dettinger MD, Caprio JM, Peterson DH. 2001. Changes in the Onset of Spring in the Western United States. *Bulletin of the American Meteorological Society* **82**(3): 399–415, DOI: 10.1175/2F1520-0477(2001)082%3C0399%3ACITOOS%3.

Chmielewski F-M, Rötzer T. 2001. Response of tree phenology to climate change across Europe. *Agricultural and Forest Meteorology* **108**: 101–112.

Chuine I, Cour P, Rousseau DD. 1999. Selecting models to predict the timing of flowering of temperate trees: implications for tree phenology modelling. *Plant, Cell & Environment* **22**: 1–13, DOI: 10.1007/s00484-004-0223-5.

Efron B. 1987. Better bootstrap confidence intervals (with discussion). *Journal of the American Statistical Association* **82**: 171–200.

Efron B, Tibshirani R. 1993. *An Introduction to the Bootstrap*. Chapman and Hall: New York.

Fitter AH, Fitter RSR. 2002. Rapid changes in flowering time in British plants. *Science* **296**: 1689–1691, DOI: 10.1126/science.1071617.

Fitter AH, Fitter RSR, Harris ITB, Williamson MH. 1995. Relationships between first flowering date and temperature in the flora of a locality in central England. *Functional Ecology* **9**: 55–60.

Grierson W. 1995. Role of temperature in the physiology of crop plants: pre- and post-harvest. In *Handbook of Plant and Crop Physiology*, Pessarakli M (ed), 2nd edn. Marcel Dekker: New York; 61–83.

Godfrey LG, Pesaran MH. 1983. Tests of non-nested regression models, small sample adjustments and Monte Carlo evidence. *Journal of Econometrics* **21**: 133–154.

Gordon C, Cooper C, Senior CA, Banks H, Gregory JM, Johns TC, Mitchell JFB, Wood RA. 2000. The simulation of SST, sea ice extents and ocean heat transports in a version of the Hadley Centre coupled model without flux adjustments. *Climate Dynamics* **16**: 147–168, DOI: 10.1007/s003820050010.

Gyalistras D. 2002. How uncertain are regional climate change scenarios? Examples for Europe and the Alps. In *Angewandte Statistik – PIK-Weiterbildungsseminar 2000/2001*, Gerstengarbe FW, PIK Report No. 75. Potsdam Institute for Climate Impact Research: Potsdam, Germany; 85–93.

Häkkinen R, Linkosalo T, Hari P. 1995. Methods for combining phenological time series: application to bud burst in birch (*Betula pendula*) in Central Finland for the period 1896-1955. *Tree Physiology* **15**: 721–726.

Häkkinen R, Linkosalo T, Hari P. 1998. Effects of dormancy and environmental factors on timing of bud burst in *Betula pendula*. *Tree Physiology* **18**: 707–712.

Harper G, Mann D, Thompson R. 2005. Phenological monitoring at Royal Botanic Garden Edinburgh. *Sibbaldia* **2**: 33–45.

Harper G, Morris L. 2006. Flowering and climate change – part 1. *Sibbaldia* **4**: 71–86.

Hastie T, Tibshirani R. 1990. *Generalized Additive Models*. Chapman and Hall: London.

Hudson IL, Keatley MR, Roberts AMI. 2005. Statistical methods in phenological research, *International Workshop in Statistical Modelling IWSM 2005*, 10-15 July. University of Western Sydney, Penrith, Sydney.

Hulme M, Jenkins GJ, Lu X, Turnpenny JR, Mitchell TD, Jones RG, Lowe J, Murphy JM, Hassell D, Boorman P, McDonald R, Hill S. 2002. *Climate change scenarios for the UK: UKCIP02 scientific report*, Tyndall Centre for Climate Change Research.

IPCC. 2007. *Climate Change 2007: The Physical Science Basis*. Cambridge University Press: Cambridge.

Jones PD, Thompson R. 2003. Instrumental records. In *Global Change in the Holocene*, Mackay AW, Battarbee RW, Birks HJB, Oldfield F (eds). Arnold: London.

Keatley MR, Hudson IL. 2007. A comparison of long-term flowering patterns of Box-Ironbark species in Havelock and Rushworth Forests. *Environmental Modelling and Assessment* **12**: 279–292, published online 9 January 2007) DOI: 10.1007/s10666-006-9063-5.

Keatley MR, Hudson IL, Fletcher TD. 2004. Long-term flowering synchrony of Box-Ironbark Eucalypts. *Australian Journal of Botany* **52**: 47–54, DOI: 10.1071/BT0317.

Kramer K. 1994. Selecting a model to predict the onset of growth of *Fagus sylvatica*. *Journal of Applied Ecology* **31**: 172–181.

Manabe S. 1970. The dependence of atmospheric temperature on the concentration of carbon dioxide. In *Proceedings of the AAAS Air Pollution Session, Dallas, Texas, Global Effects of Environmental Pollution*, Singer SF (ed). D. Reidel Publishing Co: Dordrecht; 25–29.

Manabe S, Wetherald RT. 1967. Thermal equilibrium of the atmosphere with a given distribution of relative humidity. *Journal of the Atmospheric Sciences* **24**(3): 241–259.

McCarthy JJ, Canziani OF, Leary NA, Dokken DJ, White KS (eds). 2001. *Climate Change 2001: Impacts, Adaptation and Vulnerability*. Contribution of the Working GroupII to the Third Assessment Report of the Intergovernmental Panel on Climate Change. Cambridge University Press: Cambridge.

Menzel A, Fabian P. 1999. Growing season extended in Europe. *Nature* **397**: 659.

Miller AJ. 1984. Selection of subsets of regression variables (with discussion). *Journal of the Royal Statistical Society, Series A: General* **147**: 389–425.

Myers N, Mittermeier RA, Mittermeier CG, da Fonseca GAB, Kent J. 2000. Biodiversity hotspots for conservation priorities. *Nature* **403**: 853–858, DOI: 10.1038/3500250.

Oliveira M. 1998. Calculation of budbreak and flowering base temperatures for *Vitis vinifera cv. Touriga Francesa* in the Douro Region of Portugal. *American Journal of Oenology and Viticulture* **49**: 74–78.

Parmesan C, Yohe G. 2003. A globally coherent fingerprint of climate change impacts across natural systems. *Nature* **421**: 37–42, DOI: 10.1038/nature0128.

Pesaran MH. 1982. Comparison of local power of alternative tests of non-nested regression models. *Econometrica* **50**: 1287–1306.

Penuelas J, Filella I. 2001. Responses to a warming world. *Science* **294**: 793–794. DOI: 10.1126/science.106686.

Root TL, Price JT, Hall KR, Schneider SH, Rosenzweig C, Pounds JA. 2003. Fingerprints of global warming on wild plants and animals. *Nature* **421**: 57–60, DOI: 10.1038/nature0133.

Salisbury FB. 1963. *The Flowering Process*. Pergamon Press: New York.

Saxe H, Cannell MGR, Johnsen O, Ryan MG, Vourlitis G. 2001. Tree and forest functioning in response to global warming. Tansley Review no. 123. *New Phytologist* **149**: 369–400, DOI: 10.1046/j.1469-8137.2001.00057.x.

Seber GAF. 1977. *Linear Regression Analysis*. Wiley: New York.

Sparks TH, Carey PD. 1995. The responses of species to climate over two centuries: an analysis of the Marsham phenological record, 1736-1947. *Journal of Ecology* **83**: 321–329.

Sparks TH, Carey PD, Combes J. 1997. First leafing dates of trees in Surrey between 1947 and 1996. *The London Naturalist* **76**: 15–20.

Sparks TH, Jeffree EP, Jeffree CE. 2000. An examination of the relationship between flowering times and temperature at the national scale using long-term phenological records from the UK. *International Journal of Biometeorology* **44**: 82–87, DOI: 10.1007/s004840000049.

Tanja S, Berninger F, Vesala T, Markkanen T, Hari P, Makela A, Ilvesniemi H, Hanninen H, Nikinmaa E, Huttula T, Laurila T, Aurela M, Grelle A, Lindroth A, Arneth A, Shibistova O, Lloyd J. 2003. Air temperature triggers the recovery of evergreen boreal forest photosynthesis in spring. *Global Change Biology* **9**: 1410–1426, DOI: 10.1046/j.1365-2486.2003.00597.x.

Thompson R, Clark RM. 2006. Spatio-temporal modelling and assessment of within-species phenological variability using thermal time methods. *International Journal of Biometeorology* **50**: 313–322, DOI: 10.1007/s00484-005-0017-4.

Thompson R, Clark RM. 2008. Is spring starting earlier?. *The Holocene* **18**: 95–104.

Wang JY. 1960. A critique of the heat unit approach to plant response studies. *Ecology* **41**: 785–790.

